

DTIC

✓m (2)

MTL TR 91-45

AD

AD-A243 668



# EXAMINING $\text{Si}_3\text{N}_4$ BASE MATERIALS WITH VARIOUS RARE EARTH ADDITIONS

GEORGE E. GAZZA  
CERAMICS RESEARCH BRANCH

December 1991

Approved for public release; distribution unlimited.



US ARMY  
LABORATORY COMMAND  
MATERIALS TECHNOLOGY LABORATORY

U.S. ARMY MATERIALS TECHNOLOGY LABORATORY  
Watertown, Massachusetts 02172-0001

91-18844



20000 901 030

The findings in this report are not to be construed as an official Department of the Army position, unless so designated by other authorized documents.

Mention of any trade names or manufacturers in this report shall not be construed as advertising nor as an official indorsement or approval of such products or companies by the United States Government.

#### DISPOSITION INSTRUCTIONS

Destroy this report when it is no longer needed.  
Do not return it to the originator.

UNCLASSIFIED

SECURITY CLASSIFICATION OF THIS PAGE (When Data Entered)

REPORT DOCUMENTATION PAGE		READ INSTRUCTIONS BEFORE COMPLETING FORM
1. REPORT NUMBER MTL TR 91-45	2. GOVT ACCESSION NO.	3. RECIPIENT'S CATALOG NUMBER
4. TITLE (and Subtitle) EXAMINING Si <sub>3</sub> N <sub>4</sub> BASE MATERIALS WITH VARIOUS RARE EARTH ADDITIONS		5. TYPE OF REPORT & PERIOD COVERED Final Report
		6. PERFORMING ORG. REPORT NUMBER
7. AUTHOR(s) George E. Gazza		8. CONTRACT OR GRANT NUMBER(s)
9. PERFORMING ORGANIZATION NAME AND ADDRESS U.S. Army Materials Technology Laboratory Watertown, Massachusetts 02172-0001 ATTN: SLCMT-EMC		10. PROGRAM ELEMENT, PROJECT, TASK AREA & WORK UNIT NUMBERS D/A Project: 1L162105AH84 ✓
11. CONTROLLING OFFICE NAME AND ADDRESS U.S. Army Laboratory Command 2800 Powder Mill Road Adelphi, Maryland 10783-1145		12. REPORT DATE December 1991
		13. NUMBER OF PAGES 9
14. MONITORING AGENCY NAME & ADDRESS (if different from Controlling Office)		15. SECURITY CLASS. (of this report) Unclassified
		15a. DECLASSIFICATION/DOWNGRADING SCHEDULE
16. DISTRIBUTION STATEMENT (of this Report)  Approved for public release; distribution unlimited.		
17. DISTRIBUTION STATEMENT (of the abstract entered in Block 20, if different from Report)		
18. SUPPLEMENTARY NOTES Presented at the American Ceramic Society, Cincinnati, Ohio, May 1991.		
19. KEY WORDS (Continue on reverse side if necessary and identify by block number) Silicon nitride                      Microstructure                      Creep Hot pressing                          Hardness                                  Strength Rare earths                              Oxidation		
20. ABSTRACT (Continue on reverse side if necessary and identify by block number)  (SEE REVERSE SIDE)		

UNCLASSIFIED

SECURITY CLASSIFICATION OF THIS PAGE (When Data Entered)

Block No. 20

ABSTRACT

Silicon nitride base compositions were prepared by using various rare earth oxide additives and hot pressing the powders to full density. Compositions were primarily explored in  $\text{Si}_3\text{N}_4\text{-SiO}_2\text{-RE}_2\text{Si}_2\text{O}_7$  compatibility regions although other  $\text{Si}_3\text{N}_4\text{-RE}_2\text{O}_3$  reactions were also investigated. Hot pressing densification data and high temperature behavior of the various silicon nitride-rare earth compositional systems are examined.

UNCLASSIFIED

SECURITY CLASSIFICATION OF THIS PAGE (When Data Entered)

# CONTENTS

	Page
INTRODUCTION. . . . .	1
EXPERIMENTAL. . . . .	2
MECHANICAL BEHAVIOR . . . . .	5
CREEP MEASUREMENTS. . . . .	10
OXIDATION . . . . .	15
SUMMARY AND CONCLUSIONS . . . . .	16
ACKNOWLEDGMENT. . . . .	16



Accession For	
NTIS GRA&I	<input checked="" type="checkbox"/>
DTIC TAB	<input type="checkbox"/>
Unannounced	<input type="checkbox"/>
Justification	
By	
Distribution/	
Availability Codes	
Dist	Avail and/or Special
A-1	

## INTRODUCTION

The use of various rare earth oxides as additives to promote sintering of silicon nitride is receiving greater attention in recent years.<sup>1-5</sup> In part, a renewed effort is directed toward determining whether a rare earth other than  $Y_2O_3$  can be used to densify  $Si_3N_4$  and avoid some of the problems associated with  $Y_2O_3$ -doped  $Si_3N_4$  material.<sup>6,7</sup> In addition, studies are focusing on the use of multiple rare earth oxide additions to produce duplex microstructures with high fracture toughness values.<sup>4,8</sup>

Certain material characteristics and use of preferred compositions are considered in selecting specific rare earth oxides for study as additives to  $Si_3N_4$ . Some of these characteristics are listed in Table 1. The formation of a rare earth pyrosilicate phase ( $RE_2Si_2O_7$ ) at the grain boundaries is often chosen to avoid material instability problems at intermediate temperatures (700°C to 1000°C) which are caused by the oxidation of certain phases formed by  $Si_3N_4$ -rare earth reactions. Crystallization of the pyrosilicate by a suitable heat treatment after densification of the material reduces creep and oxidation at elevated temperatures. The high temperature properties of the particular pyrosilicate phase formed are related to its melting point (refractoriness), the temperature at which it forms a eutectic with  $SiO_2$ , its crystallization behavior (degree of crystallization and crystallite size), and the thermal expansion coefficient of the boundary phase compared to the silicon nitride grains. The degree of anisotropy associated with this phase will

Table 1. RARE EARTH ADDITIVES/SILICATES:  
SOME CHARACTERISTICS CONSIDERED

- 
- |   |  |
|---|--|
| 1. Ionic radius of the rare earth (RE),                           |  |
| 2. Melting point of $RE_2Si_2O_7$ ,                               |  |
| 3. Eutectic melting point of $RE_2Si_2O_7$ - $SiO_2$ ,            |  |
| 4. Lowest eutectic in the $Si_3N_4$ - $RE_2O_3$ - $SiO_2$ system, |  |
| 5. Polymorphism of $RE_2Si_2O_7$ ,                                |  |
| 6. Crystallization behavior,                                      |  |
| 7. Thermal expansion coefficient; anisotropy and                  |  |
| 8. Valency; oxidation state                                       |  |
- 

1. HIROSAKI, N., OKADA, A., and MATOBA, K. *Sintering of  $Si_3N_4$  with the Addition of Rare Earth Oxides*. Communications of the Amer. Ceram. Soc., C-144-147, March 1988.
2. SANDERS, W. A., and MIESKOWSKI, D. M. *Strength and Microstructure of  $Si_3N_4$  with Rare Earth Oxide Additions*. Amer. Ceram. Soc. Bull., v. 64, 1985, p. 304.
3. TANI, E., NISHIJIMA, M., ICHINOSE, H., KISHI, K., and UMEBAYASHI, S. *Gas Pressure Sintering of  $Si_3N_4$  with an Oxide Addition*. Yogyo-Kyokai-Shi, v. 94, no. 2, 1986, p. 300-305.
4. TANI, E., UMEBAYASHI, S., KISHI, K., KOBAYASHI, K., and NISHIJIMA, M. *Gas-Pressure Sintering of  $Si_3N_4$  with Concurrent Addition of  $Al_2O_3$  and 5 wt% Rare Earth Oxide: High Fracture Toughness  $Si_3N_4$  with Fiber-Like Structure*. Amer. Ceram. Soc. Bull., v. 65, no. 9, 1986, p. 1311-1315.
5. HAMPSHIRE, S., LEIGH, M., MORRISSEY, V. J., POMEROY, M. J., and SARUHAN, B. *Crystallization Heat Treatments of Silicon Nitride Ceramics and Glass-Ceramics Containing Neodymia*. Proc. 3rd Internat. Symp. on Ceramic Materials and Components for Engines, Las Vegas, NV, November 1988, p. 432-442.
6. PATEL, J. K., and THOMPSON, D. P. *The Low Temperature Oxidation Problem in Yttria-Densified Silicon Nitride Ceramics*. Br. Ceram. Trans. J., v. 87, 1988, p. 70-73.
7. LANGE, F. F., SINGHAL, S. C., and KUZNICKI, R. C. *Phase Relations and Stability Studies in the  $Si_3N_4$ - $SiO_2$ - $Y_2O_3$  Pseudoternary System*. J. Amer. Ceram. Soc., v. 60, 1977, p. 249-252.
8. LI, C. W., YAMANIS, J., WHALEN, P. J., GASDASKA, C. J., and BALLARD, C. P. *In Situ Reinforced Silicon Nitride Ceramics*. The 37th Sagamore Army Materials Research Conference Proceedings: Structural Ceramics, Plymouth, MA, 1990, p. 284-293.

also influence properties. Other criteria used for the selection of a particular rare earth are its characteristic valency (single or variable valency) or the ionic radius of the cation. In the rare earth series, the ionic radius of the cation decreases (also the size of the unit cell) with increasing atomic number. This is known as the lanthanide contraction.

In a study conducted by Andersson and Bratton,<sup>9</sup> the influence of this effect on the high temperature strength (modulus of rupture) of hot-pressed silicon nitride compositions doped with various rare earth additives was examined. Standard compositions contained approximately 6.5 m/o rare earth oxide and 13.0 m/o  $\text{SiO}_2$ . Rare earths used in the study were  $\text{Yb}_2\text{O}_3$ ,  $\text{Er}_2\text{O}_3$ ,  $\text{Sc}_2\text{O}_3$ ,  $\text{Y}_2\text{O}_3$ ,  $\text{La}_2\text{O}_3$ ,  $\text{Ce}_2\text{O}_3$ ,  $\text{Pr}_2\text{O}_3$ ,  $\text{Nd}_2\text{O}_3$ ,  $\text{Sm}_2\text{O}_3$ ,  $\text{Gd}_2\text{O}_3$ , and  $\text{Dy}_2\text{O}_3$ . They found that the high temperature strength increased with decreasing ionic radius of the rare earth additive and suggested that corresponding decreases in the bond length of the silicates formed may be responsible for improving the high temperature properties.

Since it was of interest to determine whether this effect would influence the high temperature time-dependent properties (creep) or other properties, such as strength and hardness, the present study was conducted using rare earths with relatively small ionic radii as additives to determine both the room temperature and high temperature (1200°C to 1400°C) properties of the resultant materials.

## EXPERIMENTAL

The silicon nitride starting powder selected for use in the study was TOSOH TS-10. The powder is approximately 95% to 96% alpha phase. Rare earths obtained for use as additives were  $\text{Sc}_2\text{O}_3$ ,  $\text{Lu}_2\text{O}_3$ ,  $\text{Yb}_2\text{O}_3$ ,  $\text{Er}_2\text{O}_3$ , and  $\text{Dy}_2\text{O}_3$ . Chemical analyses of the starting materials and their supply source are shown in Table 2. The purity level of the additives is essentially 99.9%.

The additives were milled with the silicon nitride powder and a small amount of silica in a nylon jar with hot isostatically pressed  $\text{Si}_3\text{N}_4$  milling balls in isopropanol for 18 hours. Compositions with each rare earth additive were prepared to produce a standard composition of 90.0 m/o  $\text{Si}_3\text{N}_4$ -3.0 m/o rare earth oxide-7.0 m/o  $\text{SiO}_2$ . This composition was located on the  $\text{SiO}_2$  rich side of the  $\text{Si}_3\text{N}_4$ - $\text{Y}_2\text{Si}_2\text{O}_7$  tie line in the  $\text{Si}_3\text{N}_4$ - $\text{Y}_2\text{O}_3$ - $\text{SiO}_2$  phase diagram. The milled powder mixtures were dried and hot pressed in graphite dies at 25 MPa uniaxial pressure, under 0.1 MPa nitrogen, for 120 minutes at final hot pressing temperatures within the 1790°C to 1805°C range. Bars 3 mm x 4 mm x 46 mm were machined from hot-pressed discs approximately 63.5 mm diameter x 8.0 to 9.0 mm thick. Immersion densities were determined with the machined bars for each  $\text{Si}_3\text{N}_4$ -rare earth additive composition. The mean values are listed in Table 3.

Pieces from machined bars were powdered and analyzed by XRD. The phase compositions formed with the  $\text{Er}_2\text{O}_3$ ,  $\text{Lu}_2\text{O}_3$ , and  $\text{Yb}_2\text{O}_3$  additives were comprised of beta- $\text{Si}_3\text{N}_4$ ,  $\text{Si}_2\text{N}_2\text{O}$ , and the pyrosilicate of the respective additive used, i.e.,  $\text{Er}_2\text{Si}_2\text{O}_7$ ,  $\text{Lu}_2\text{Si}_2\text{O}_7$ , or  $\text{Yb}_2\text{Si}_2\text{O}_7$ . A small amount of alpha- $\text{Si}_3\text{N}_4$  also appeared to be present in the  $\text{Er}_2\text{O}_3$  and  $\text{Lu}_2\text{O}_3$ -doped materials. The  $\text{Dy}_2\text{O}_3$ -doped  $\text{Si}_3\text{N}_4$  may have had a glassy grain boundary phase in that the XRD results did not indicate the presence of crystalline phases other than beta- $\text{Si}_3\text{N}_4$  and  $\text{Si}_2\text{N}_2\text{O}$ .

9. ANDERSSON, C. A., and BRATTON, R. *Ceramic Materials for High Temperature Turbines*. U.S. Energy Res. Dev. Adm. Contract Ey-76-C-05-5210, Final Report, 1977.

Table 2. CHEMICAL ANALYSES OF STARTING MATERIALS (Wt%)  
(SUPPLIERS ANALYSIS)

Si <sub>3</sub> N <sub>4</sub> TOSOH TS-10	Rare Earth Oxides (99.9%)				
	Dy <sub>2</sub> O <sub>3</sub> *	Yb <sub>2</sub> O <sub>3</sub> *	Er <sub>2</sub> O <sub>3</sub> †	Lu <sub>2</sub> O <sub>3</sub> †	Sc <sub>2</sub> O <sub>3</sub> ‡
N-38.0	Gd-0.04	Gd-0.03	Ho-0.01	Yb-0.05	Yb-0.01
O-1.0	Ho-0.01	Tb-0.01	Si-0.01	Si-0.01	Y-0.01
C-0.06	Y-0.03	Dy-0.01	Fe-0.01	Fe-0.01	Ca-0.005
Cl-0.03		Y-0.03	Mg-0.01	Mg-0.01	
Fe-0.01			Ca-0.01	Ca-0.01	
			Al-0.01	Al-0.01	

\*Molycorp Inc., Louviers, CO

†Research Chemicals, Phoenix, AZ

‡Johnson Matthey Alpha, Ward Hill, MA

Table 3. MATERIAL COMPOSITION, HOT-PRESSED DENSITY,  
AND DENSIFICATION PARAMETERS

Composition	Density (g/cc)
90 m/o Si <sub>3</sub> N <sub>4</sub> + 3.0 m/o Dy <sub>2</sub> O <sub>3</sub> + 7.0 m/o SiO <sub>2</sub>	3.320
90 m/o Si <sub>3</sub> N <sub>4</sub> + 3.0 m/o Er <sub>2</sub> O <sub>3</sub> + 7.0 m/o SiO <sub>2</sub>	3.346
90 m/o Si <sub>3</sub> N <sub>4</sub> + 3.0 m/o Yb <sub>2</sub> O <sub>3</sub> + 7.0 m/o SiO <sub>2</sub>	3.349
90 m/o Si <sub>3</sub> N <sub>4</sub> + 3.0 m/o Lu <sub>2</sub> O <sub>3</sub> + 7.0 m/o SiO <sub>2</sub>	3.357
90 m/o Si <sub>3</sub> N <sub>4</sub> + 3.0 m/o Sc <sub>2</sub> O <sub>3</sub> + 7.0 m/o SiO <sub>2</sub>	3.195

Densification Parameters

Applied Pressure - 25 MPa

Final Hot Pressing Temperature Range - 1790°C to 1805°C

Hot Pressing Time at Final Temperature - 120 Minutes



The densification behavior of the powders was studied by monitoring the shrinkage during the hot pressing run. In particular, for each composition, the temperatures at which the onset of rapid shrinkage occurs were noted as these temperatures should approximate when liquid first forms in the reacting powder mixture, that is, when the temperature approaches that of the lowest eutectic in the compositional system. These temperatures are listed in Table 4 along with the incipient melting points (lowest melting eutectics) found by Andersson et al.<sup>9</sup> by heating compacted powder mixtures of  $\text{Si}_3\text{N}_4$ ,  $\text{SiO}_2$ , and various rare earth oxides. Where melting was not observed up to the temperature shown in the table, the incipient melting points were indicated to be greater than this temperature. Also shown are temperatures reported for the melting point of the various pyrosilicate phases for rare earths used in the study and melting points of the pyrosilicate- $\text{SiO}_2$  eutectic. Reasonable agreement appears to exist between the incipient melting points found by Andersson et al.<sup>9</sup> for their  $\text{Si}_3\text{N}_4$ - $\text{SiO}_2$  rare earth oxide mixtures and the temperatures at which the onset of rapid shrinkage occurs for the corresponding  $\text{Si}_3\text{N}_4$ - $\text{SiO}_2$  rare earth oxide powders hot pressed in this study.

Table 4. COMPARISON OF MELTING POINT TEMPERATURES WITH ONSET OF SHRINKAGE TEMPERATURES DURING HOT PRESSING OF  $\text{Si}_3\text{N}_4$ - $\text{RE}_2\text{O}_3$ - $\text{SiO}_2$  COMPOSITIONAL SYSTEMS

Rare Earth Additive	Melting Point of $\text{RE}_2\text{Si}_2\text{O}_7^*$ (°C)	Melting Point of the $\text{RE}_2\text{Si}_2\text{O}_7^*$ Eutectic <sup>†</sup> (°C)	Est. Lowest Eut. in the $\text{Si}_3\text{N}_4$ $\text{RE}_2\text{Si}_2\text{O}_3$ - $\text{SiO}_2$ System (°C)	Temp. Onset of Shrinkage During Hot Pressing <sup>‡</sup> (°C)
$\text{Dy}_2\text{O}_3$	1720 (I)	1640	1550/1570	1565-1575
$\text{Er}_2\text{O}_3$	1800 (C)	1680	>1625	1630-1640
$\text{Yb}_2\text{O}_3$	1850 (C)	1650	>1565	1595-1605
$\text{Lu}_2\text{O}_3$	1850 (C)	---	---	1675-1685
$\text{Sc}_2\text{O}_3$	1850 (C)	1660	>1675	1725-1735
$\text{Y}_2\text{O}_3$	1775 (I)	1660	1580	1570-1580

\*Data from Handbook of Phase Diagrams of Silicate Systems, v. 1, N. A. Toropov, V. P. Barzakovskii, V. V. Lapin, N. N. Kurtseva. U.S. Department of Commerce, Natl. Tech. Information Service, Springfield, VA 22151

<sup>†</sup>Data from Ceramic Materials for High Temperature Turbines, C. A. Andersson and R. J. Bratton, Final Report. ERDA E-76-C-05-5210, 1977

<sup>‡</sup>Heating Rate During Hot Pressing - 10°C/Minute (Present Study)

I = Incongruent Melting

C = Congruent Melting

## MECHANICAL BEHAVIOR

Bars machined from the hot-pressed discs were used to determine room temperature modulus of rupture (MOR) and high temperature creep and oxidation resistance. MOR testing was conducted in four-point bending on fixtures with a 20 mm loading span on the compressive surface and a 40 mm load span on the tensile surface. Platen rate was 0.5 mm/minute. Results obtained from the MOR tests are shown in Table 5. The data was generated with specimens as-machined from the hot-pressed discs and with specimens that had been used in high temperature creep tests. In the latter case, it was of interest to determine the retained strength of specimens after they had been exposed to high temperature creep conditions (to be described later in the report).

Table 5. MODULUS OF RUPTURE DETERMINED AT ROOM TEMPERATURE WITH SPECIMENS AS-MACHINED FROM HOT-PRESSED MATERIALS AND WITH SPECIMENS USED FOR HIGH TEMPERATURE CREEP TESTS

Rare Earth Additive	Specimens As-Machined From Hot-Pressed Material	Retained MOR on Specimens Used For Creep Tests		
	MOR (MPa)	MOR (MPa)	Test Temp. (°C) (For Creep)	Permanent Strain (%)
Dy <sub>2</sub> O <sub>3</sub>	High-810	828	1250	0.12
	Mean-751	668	1300	0.30
	Low-698	988	1350	0.95
Er <sub>2</sub> O <sub>3</sub>	High-832	770	1250	0.13
	Mean-760	757	1300	0.29
	Low-712	540	1350	0.78
		867	1300	0.21*
		653	1350	0.51†
Yb <sub>2</sub> O <sub>3</sub>	High-762	852	1200	0.14
	Mean-706	792	1250	0.26
	Low-648	645	1300	0.60
Lu <sub>2</sub> O <sub>3</sub>	High-860	790	1300	0.10
	Mean-773	718	1300	0.12
	Low-683	670	1350	0.30
		712	1400	0.65
		472	1400	0.49‡
Sc <sub>2</sub> O <sub>3</sub>	---	843	1250	0.21
	---	803	1300	0.30
	---	613	1350	0.42

\*Creep tested for 166 hours

†Creep tested for 195 hours

‡Creep tested for 182 hours

For specimens tested in the as-machined condition, mean, high and low MOR values are shown in Table 5 for each composition. The mean values ranged from 706 to 773 MPa for the  $\text{Si}_3\text{N}_4\text{-Yb}_2\text{O}_3\text{-SiO}_2$  material and the  $\text{Si}_3\text{N}_4\text{-Lu}_2\text{O}_3\text{-SiO}_2$  material, respectively. Some MOR values higher than 800 MPa were observed for  $\text{Dy}_2\text{O}_3$ ,  $\text{Er}_2\text{O}_3$ , and  $\text{Lu}_2\text{O}_3$ -doped specimens.

Retained MOR (at room temperature) was determined for specimens that had been creep tested. The temperature at which these specimens had been tested along with the amount of permanent strain (as a result of creep) measured on each specimen are shown in the table with each MOR value. Some high values, 888, 867, 852, and 843 MPa were noted for the  $\text{Dy}_2\text{O}_3$ ,  $\text{Er}_2\text{O}_3$ , and  $\text{Sc}_2\text{O}_3$ -doped compositions, respectively. Lower values were obtained, in general, when increasing temperatures were used for the creep tests or with increasing permanent strain in the bar.

Using geometrical analysis, a 1.0% strain value would be equivalent to a curvature/specimen thickness ratio of 50 for the specimen and load span dimensions used in the MOR tests. Since the bars tested had permanent strain values of <1.0%, the curvature/specimen thickness ratio would be >50. Errors associated with testing curved specimens have been shown to be small (<1%) from curved beam analysis<sup>10</sup> when the curvature specimen thickness ratio is large (>40).

Fracture surfaces of  $\text{Si}_3\text{N}_4$  specimens doped with  $\text{Lu}_2\text{O}_3$ ,  $\text{Er}_2\text{O}_3$ ,  $\text{Yb}_2\text{O}_3$ , and  $\text{Sc}_2\text{O}_3$  are shown in Figures 1a, 1b, 2a, and 2b, respectively. The microstructures are typical of hot-pressed  $\text{Si}_3\text{N}_4$  material where the conversion of alpha to beta phase forms high aspect grains by solution reprecipitation through a liquid phase produced from  $\text{Si}_3\text{N}_4$ -additive reactions. Grain diameters are in the 1 to 2  $\mu\text{m}$  range. Fracture strengths shown in Table 5 were limited by the presence of iron impurity found at the fracture origin of most specimens. Typically, the affected area appears as a dark spot in the material and is observed in Figures 3a and 3b, the fracture origin of a  $\text{Yb}_2\text{O}_3$ -doped  $\text{Si}_3\text{N}_4$  specimen. In Figure 3a, the affected area is approximately 35 to 40  $\mu\text{m}$  in size resulting in a specimen MOR value of 707 MPa. At higher magnification, Figure 3b, the coarsening of the microstructure produced by the Fe impurity is observed surrounded by a finer grain structure.

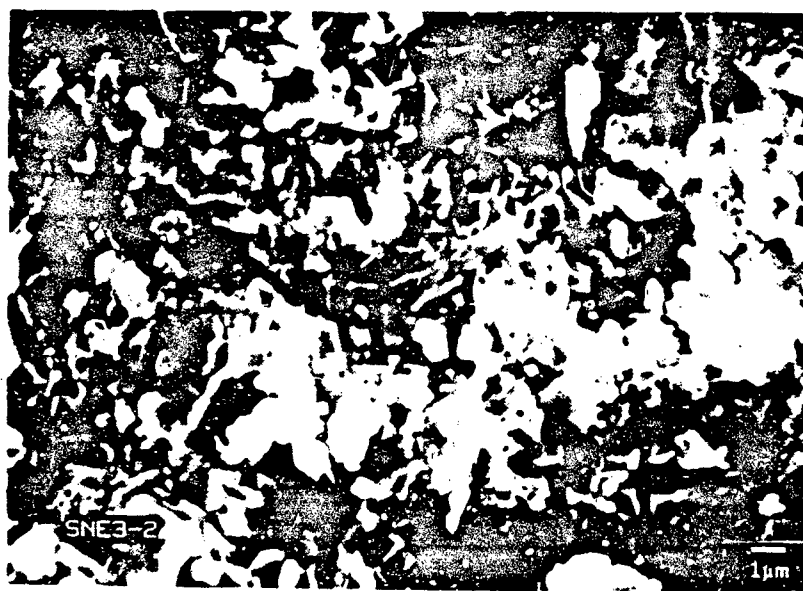
The hardness, indentation fracture toughness, and elastic modulus of the materials were measured and listed in Table 6. The hardness was determined using a Vickers indenter under a 2 kg load. The  $\text{Sc}_2\text{O}_3$ -doped composition had the highest hardness while  $\text{Yb}_2\text{O}_3$  and  $\text{Dy}_2\text{O}_3$ -doped material had the lowest values. It is uncertain whether the higher hardness values found for the  $\text{Sc}_2\text{O}_3$ ,  $\text{Lu}_2\text{O}_3$ , and  $\text{Er}_2\text{O}_3$ -doped  $\text{Si}_3\text{N}_4$  materials were affected by the presence of residual alpha phase  $\text{Si}_3\text{N}_4$ . Indentation fracture toughness was calculated using a technique reported by Niihara et al.<sup>11</sup> Indentation loads applied were 11 kg. Fracture toughness values were calculated using both median and Palmqvist cracks. The crack length/indentation size ratio favored the use of the Palmqvist expression and these values are listed in Table 6. The  $\text{Er}_2\text{O}_3$  and  $\text{Lu}_2\text{O}_3$ -doped compositions gave the highest toughness values. Although not reported here, when the equation for median cracks was used, higher fracture toughness values were calculated for all compositions. Elastic moduli were derived from ultrasonic measurements. Again, except for the  $\text{Yb}_2\text{O}_3$ -doped material, higher values appeared to be favored by doping with rare earths having smaller ionic radii.

10. BARATTA, F. L., MATTHEWS, W. T., and QUINN, G. D. *Errors Associated with Flexure Testing of Brittle Materials*. U.S. Army Materials Technology Laboratory, MTL TR 87-35, July 1987.

11. NIIHARA, K., MORENA, R., and HASSELMAN, D. P. H. *Further Reply to Comment on Elastic/Plastic Indentation Damage in Ceramics: The Median/Radial Crack System*. Communications of the Amer. Ceramic Soc., C-116, July 1982.



a.  $\text{Lu}_2\text{O}_3$

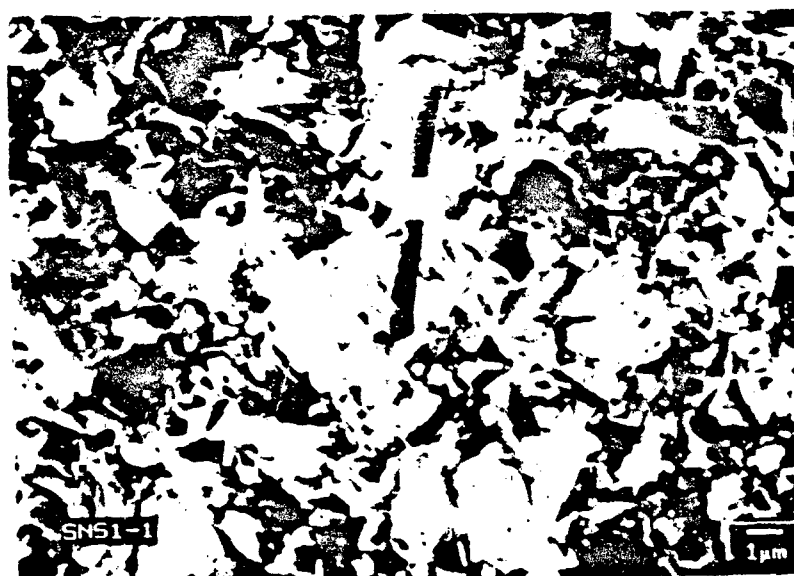


b.  $\text{Er}_2\text{O}_3$

Figure 1. Fracture surfaces of doped  $\text{Si}_3\text{N}_4$  specimens. Mag. 5000X



a.  $\text{Yb}_2\text{O}_3$

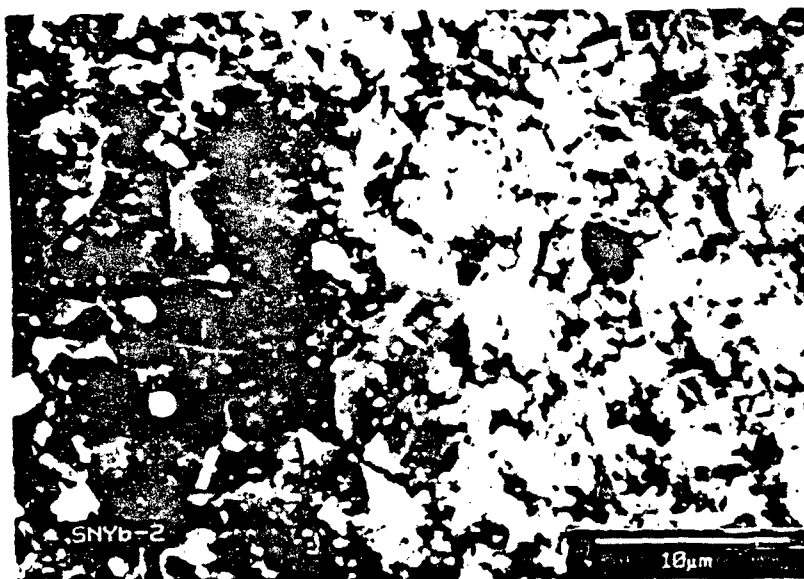


b.  $\text{Sc}_2\text{O}_3$

Figure 2. Fracture surfaces of doped  $\text{Si}_3\text{N}_4$  specimens. Mag. 5000X



a. A 25 to 30  $\mu\text{m}$  Impurity (Fe) Affected Region. Mag. 800X



b. Boundary Between Coarsened Region and Finer Grained Matrix. Mag. 2780X

Figure 3. Fracture origin in  $\text{Yb}_2\text{O}_3$ -doped  $\text{Si}_3\text{N}_4$  specimens.

Table 6. HARDNESS, INDENTATION FRACTURE TOUGHNESS, AND ELASTIC MODULUS OF HOT-PRESSED  $\text{Si}_3\text{N}_4\text{-RE}_2\text{O}_3\text{-SiO}_2$  COMPOSITIONS

Rare Earth Additive	Hardness* (VHN) (GPa)	Fracture Toughness† (MPam)	Elastic Modulus‡ (GPa)
$\text{Dy}_2\text{O}_3$	16.1	5.53	303
$\text{Yb}_2\text{O}_3$	16.5	5.76	307
$\text{Er}_2\text{O}_3$	17.5	6.85	309
$\text{Lu}_2\text{O}_3$	17.5	6.86	315
$\text{Sc}_2\text{O}_3$	19.0	5.70	318

\*2 kg load

†11 kg load

‡Ultrasonic Method

#### CREEP MEASUREMENTS

The objective of the high temperature, time-dependent study was limited to determining the extent of permanent strain that would develop in the bars under a constant stress (300 MPa) at temperatures between 1200°C and 1400°C for times up to approximately 350 hours. Machined bars were loaded in four-point bending on SiC fixtures with the same loading span dimensions as the room temperature fixtures. The bars were placed under static loading calculated to produce 300 MPa flexural stress. Testing temperatures used were between 1200°C and 1400°C with time under stress approximately 350 hours for most specimens although, in some cases, shorter times, 185 to 195 hours, were chosen to produce other time-dependent values of permanent strain in the bars. All testing was conducted in an air environment. After the required number of hours under stress and temperature had elapsed, the specimens were unloaded and cooled to room temperature for permanent strain measurements and weight gain determinations. Strain measurements were performed using a method reported by Hollenberg et al.<sup>12</sup> The formula used is based on measuring specimen curvature, shown in Figure 4. Permanent strain,  $\epsilon$ , was derived from measurements on the bars where  $L$  is the distance between top loading points,  $t$  is the bar thickness, and  $Y$  is the rise generated by the arc formed by the specimen curvature and the chord subtended by that arc. Dimensional measurements used for the calculations were taken on the creep tested specimens with a stereoscope. Limitations of the method are that the strain is restricted to 1 to 1.5% maximum, the curvature is reasonably uniform, and the creep properties in tension and compression are similar, that is, the neutral axis is not displaced.

Specimens tested in this study did not produce strains greater than 1% and measurements along the curved surfaces indicated the curvature to be reasonably uniform between the loading points. The similarity of creep behavior in tension and compression was determined by measuring curvature on both tensile and compressive surfaces and calculating the permanent strain values. These are compared in

12. HOLLENBERG, G. W., TERWILLIGER, G. R., and GORDON, R. S. *Calculation of Stresses and Strains in Four-Point Bending Creep Tests*. J. Amer. Ceram. Soc., 1971, p. 196-199.

$$\text{Permanent Strain (e)} = \frac{4 (t) (Y)}{(L)^2}$$

Figure 4. Schematic diagram for permanent strain measurement in flexure specimen.

Table 7 for several different compositions exposed to test temperatures of 1300°C to 1400°C for approximately 350 hours. The strain values are within 0.03% for a given test specimen. A complete listing of permanent strain values determined in this investigation is shown in Table 8. For each rare earth-doped  $\text{Si}_3\text{N}_4$  composition, the permanent strain value shown (%) was determined for a specimen of that composition tested at a temperature indicated at the top of the column. The actual duration of the test, in hours, is indicated by the number enclosed in parentheses under the strain value. Also shown are permanent strain determinations for  $\text{Er}_2\text{O}_3$ -doped  $\text{Si}_3\text{N}_4$  and  $\text{Lu}_2\text{O}_3$ -doped  $\text{Si}_3\text{N}_4$  held for shorter times at temperature and for specimens of these compositions which were prefired in nitrogen at 1300°C for eight hours attempting to promote further crystallization of the grain boundary prior to creep testing. A commercially available material, Kyocera grade 252, an in situ toughened  $\text{Si}_3\text{N}_4$  doped with  $\text{Yb}_2\text{O}_3$  (and small amounts of  $\text{Y}_2\text{O}_3$  and  $\text{Al}_2\text{O}_3$ ) was included in the study for comparative purposes. As expected, for each composition, the amount of permanent strain increased with increasing test temperature. The specimens of  $\text{Lu}_2\text{O}_3$ -doped  $\text{Si}_3\text{N}_4$  that were prefired in nitrogen had a similar amount of permanent strain as the as-hot-pressed specimens after testing at temperatures of 1300°C and 1350°C. This may be due to a significant amount of crystallization already occurring during the cooldown from the hot pressing temperature for this composition. However, the specimens of  $\text{Er}_2\text{O}_3$ -doped  $\text{Si}_3\text{N}_4$  prefired in nitrogen showed a reduction in permanent strain as compared with as-hot-pressed material. At 1300°C, the permanent strain was reduced from 0.29% to 0.23% and at 1350°C from 0.78% to 0.59%.

Table 7. COMPARISON OF PERMANENT STRAIN MEASUREMENTS ON THE COMPRESSION AND TENSILE SURFACES

Rare Earth Additive	Test Temp. (°C)	Perm. Strain (%) (Compressive)	Perm Strain (%) (Tensile)
$\text{Dy}_2\text{O}_3$	1350	0.95	0.92
$\text{Er}_2\text{O}_3$	1350	0.59	0.57
$\text{Lu}_2\text{O}_3$	1350	0.27	0.28
$\text{Lu}_2\text{O}_3$	1400	0.65	0.63
Kyocera 252*	1300	0.43	0.46

\*A high toughness  $\text{Yb}_2\text{O}_3$ -doped  $\text{Si}_3\text{N}_4$  containing small amounts of  $\text{Y}_2\text{O}_3$  and  $\text{Al}_2\text{O}_3$ . (Kyocera Corp., Japan)



Table 8. PERMANENT STRAIN IN  $\text{Si}_3\text{N}_4\text{-RE}_2\text{O}_3\text{-SiO}_2$  COMPOSITIONS AFTER APPROXIMATELY 350 HOURS UNDER 300 MPa FLEXURE STRESS AT TEMPERATURES OF 1200°C to 1400°C

Rare Earth Additive	Temperature (°C)				
	1200	1250	1300	1350	1400
$\text{Yb}_2\text{O}_3$	0.14% (355)	0.26% (351)	0.60% (355)	---	---
$\text{Dy}_2\text{O}_3$	---	0.12% (354)	0.30% (356)	0.95% (355)	---
$\text{Sc}_2\text{O}_3$	---	0.21% (355)	0.30% (353)	0.42% (354)	---
$\text{Er}_2\text{O}_3$	---	0.13% (353)	0.23% (351)	0.78% (352)	---
$\text{Er}_2\text{O}_3$	---	---	0.21% (166)	0.51% (192)	---
$\text{Er}_2\text{O}_3^*$	---	---	0.23% (355)	0.59% (355)	---
$\text{Lu}_2\text{O}_3$	---	---	0.10% (352)	0.30% (352)	0.65% (345)
$\text{Lu}_2\text{O}_3$	---	---	---	---	0.49% (188)
$\text{Lu}_2\text{O}_3^*$	---	---	0.12% (355)	0.27% (355)	---
Kyocera 252	---	0.19% (355)	0.44% (355)	0.98% (353)	---

\*Specimen pre-fired in  $\text{N}_2$  at 1300°C for 8 hours before creep testing.

NOTE: Numbers in parenthesis, beneath strain values, represent the actual test duration times (hours).

The data may be graphically represented by a semilogarithmic plot of permanent strain versus temperature, illustrated in Figure 5. Plots of data for  $\text{Si}_3\text{N}_4$  doped with  $\text{Dy}_2\text{O}_3$ ,  $\text{Yb}_2\text{O}_3$ ,  $\text{Er}_2\text{O}_3$ , or  $\text{Lu}_2\text{O}_3$  appear to have reasonably similar slopes suggesting a common mechanism for producing time-dependent strain at high temperatures in these materials. Only the  $\text{Sc}_2\text{O}_3$ -doped  $\text{Si}_3\text{N}_4$  exhibits a significantly different slope. However, further testing and characterization of this material is required. The  $\text{Lu}_2\text{O}_3$ -doped material clearly shows the highest resistance to strain of the materials tested.

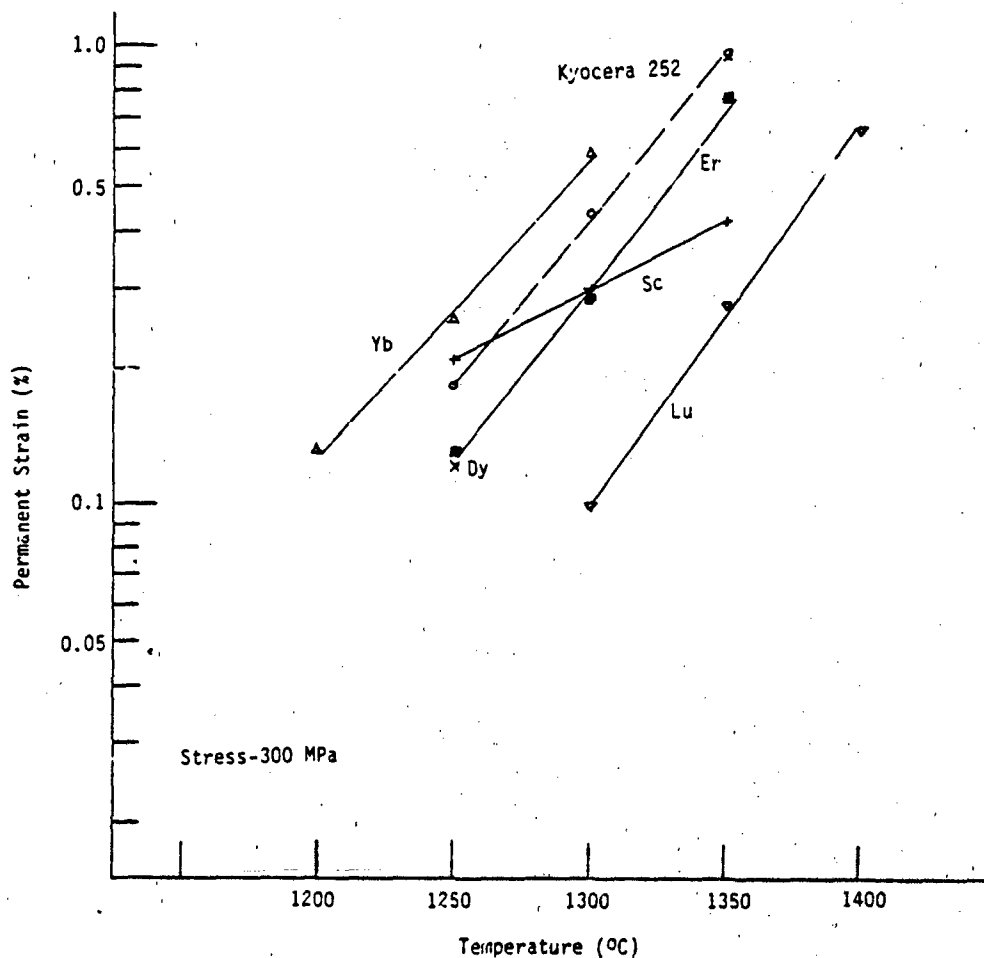


Fig. 5. Permanent strain (%) versus temperature for  $\text{Si}_3\text{N}_4\text{-RE}_2\text{O}_3\text{-SiO}_2$  compositions tested under 300 MPa flexure stress for approximately 350 hours.

The bars were analyzed by XRD to determine the phases existing after the long exposure to high temperature during creep testing. All specimens showed beta- $\text{Si}_3\text{N}_4$  and  $\text{Si}_2\text{N}_2\text{O}$  to be present. The compounds  $\text{Lu}_2\text{Si}_2\text{O}_7$ ,  $\text{Yb}_2\text{Si}_2\text{O}_7$ ,  $\text{Er}_2\text{Si}_2\text{O}_7$ , and  $\text{Sc}_2\text{Si}_2\text{O}_7$  were also found in specimens doped with their respective oxides. Peak intensities for these pyrosilicate phases were significantly greater than found in the as-hot-pressed materials indicating that appreciable crystallization of these phases had occurred during high temperature testing. In the  $\text{Dy}_2\text{O}_3$ -doped specimens, the presence of a phase which appeared analogous to the  $\text{Y}_5(\text{SiO}_4)_3\text{N}$

(nitrogen-apatite) phase formed during high temperature testing rather than the expected pyrosilicate phase. Apparently, a compositional shift occurred during hot pressing which was not detected until crystallization of the phase occurred during the high temperature tests. The development of this phase, which appears to be dysprosium N-apatite, at the grain boundaries may increase resistance to high temperature creep over  $\text{Dy}_2\text{Si}_2\text{O}_7$  containing material. Oxidation of the  $\text{Dy}_2\text{O}_3$ -doped material at 900°C and 1000°C did not indicate the existence of any intermediate temperature problems. However, the oxidation studies were conducted with as-hot-pressed specimens, before crystallization of this phase was observed.

Creep behavior in silicon nitride is primarily governed by viscous flow of the grain boundary phase, grain boundary sliding/cavitation, or diffusional processes.<sup>13-15</sup> In flexure, the creep behavior of  $\text{Si}_3\text{N}_4$  has been described as transient<sup>16</sup> rather than attaining steady state conditions. Determination of creep mechanisms usually involves calculations of activation energy and stress exponents based on the temperature and stress dependence of the strain (creep) rate accompanied by TEM to observe microstructural changes in the specimens. It was not an objective of this study to suggest creep mechanisms responsible for the development of permanent strain observed in the test specimens. However, from the permanent strain data available, activation energies were calculated from log strain rate versus  $1/T$ . Strain rate values were derived from permanent strain versus time data. From the calculations, based on the data used to construct Figure 5, it was determined that the activation energies fell between 70 and 100 kcal/mol for all compositions except for the  $\text{Sc}_2\text{O}_3$ -doped  $\text{Si}_3\text{N}_4$ . These values are lower than would be obtained under steady-state conditions because the total strain values used represent cumulative strain from both primary and secondary stages of creep. The activation energy value rises to approximately 140 kcal/mol if only the strain data obtained after testing  $\text{Er}_2\text{O}_3$ -doped  $\text{Si}_3\text{N}_4$  specimens for 166 and 351 hours at 1300°C and 192 and 352 hours at 1350°C (data from Table 8) is used for the calculation. This value would essentially be associated with creep behavior in the secondary stage (steady-state region) of the creep test. Activation energies of this magnitude have been reported for a suggested mechanism of creep deformation by viscous flow with strain accommodation by grain boundary sliding.<sup>14,15</sup> This may be related to the existence of an amorphous layer between the  $\text{Si}_3\text{N}_4$  grains and the crystalline phase formed in the boundaries, as observed by Kleebe and Ruhle<sup>17</sup> and Clarke.<sup>18</sup> As the boundary phase crystallizes, the composition of the amorphous phase formed should be driven toward a eutectic composition in the system.<sup>19</sup> Mechanical behavior, particularly at high temperature, would be significantly influenced by the thickness and composition of the amorphous phase layer as well as the structure and composition of the crystalline

13. KOSSOWSKY, R., MILLER, D. G., and DIAZ, E. S. *Tensile and Creep Strengths of Hot-Pressed  $\text{Si}_3\text{N}_4$* . J. Matls. Sci., v. 10, 1975, p. 983-997.
14. SELTZER, M. S. *High Temperature Creep of Silicon-Base Compounds*. Amer. Ceram. Soc. Bull., v. 56, no. 4, 1977, p. 418-423.
15. MOSHER, D. R., RAJ, R., and KOSSOWSKY, R. *Measurement of Viscosity of the Grain Boundary Phase in Hot-Pressed Silicon Nitride*. J. Matls. Sci., v. 11, 1976, p. 49-53.
16. WIEDERHORN, S. M., and TIGHE, N. J. *Structural Reliability of Yttria-Doped Hot-Pressed Silicon Nitride at Elevated Temperatures*. J. Amer. Ceram. Soc., v. 66, no. 12, 1983, p. 884-889.
17. KLEEBE, H.-J., and RUHLE, M. *High Resolution Electron Microscopy Studies on Crystalline Secondary Phases in Silicon Nitride Based Materials*. Presented at the 93rd Annual Amer. Ceramic Society Meeting, Cincinnati, OH, 30 April 1991.
18. CLARKE, D. R. *The Microstructure of Nitrogen Ceramics in Progress in Nitrogen Ceramics*, Proc. of the NATO Adv. Study Inst. on Nitrogen Ceramics, Univ. of Sussex, U.K., July 27 - August 7, 1981, F. L. Riley, ed., M. Nijhoff, Pub., 1983, p. 341-357.
19. LANGE, F. F. *Importance of Phase Equilibria on Process Control of  $\text{Si}_3\text{N}_4$  Fabrication in Ceramics for High Performance Applications III-Reliability*, Proc. of the 6th Army Materials Technology Conf., Orcas Island, WA, July 10-13, 1979, E. M. Lenoe, R. N. Katz, and J. J. Burke, eds., Intenum Press, NY, 1983, p. 275-291.

phase(s) formed in the grain boundaries and at triple points. The solubility of nitrogen in these grain boundary phases is unknown and its effect on eutectic temperatures as well as resultant mechanical behavior, such as creep, needs clarification. It was noted that the  $\text{Si}_3\text{N}_4$ -rare earth compositions with increasing creep resistance were similar in order to the compositions having higher onset of shrinkage temperatures during hot pressing.

## OXIDATION

Oxidation measurements were made with unstressed test bars fired in air at 900°C and 1000°C and from bars used for the creep testing at 1200°C to 1400°C. All bars were weighed to the nearest 0.1 mg before exposure to high temperatures. The unstressed  $\text{Si}_3\text{N}_4$  specimens doped with  $\text{Dy}_2\text{O}_3$ ,  $\text{Yb}_2\text{O}_3$ ,  $\text{Er}_2\text{O}_3$ , and  $\text{Lu}_2\text{O}_3$  had negligible weight gains (0.1 mg max.) after 41 hours at 900°C and 192 hours at 1000°C. The specimens used for creep testing were reweighed after the tests and weight gains observed ( $\text{mg}/\text{cm}^2$ ) are shown in Table 9. Time at temperature was approximately 350 hours. Excellent resistance to oxidation at all temperatures is indicated for each composition. The  $\text{Sc}_2\text{O}_3$ -doped material shows somewhat higher weight gains than the other compositions but the values are reasonably consistent with those reported by Cheong and Sanders<sup>20</sup> for material of similar composition.

Table 9. OXIDATION OF  $\text{Si}_3\text{N}_4$ - $\text{RE}_2\text{O}_3$ - $\text{SiO}_2$  COMPOSITIONS  
(WEIGHT GAIN AFTER CREEP TESTS -  $\text{mg}/\text{cm}^2$ )

Rare Earth Additive	Temperature (°C)				
	1200	1250	1300	1350	1400
$\text{Dy}_2\text{O}_3$	—	0.08	0.12	0.13	—
$\text{Er}_2\text{O}_3$	—	0.06	0.09	0.13	—
$\text{Yb}_2\text{O}_3$	0.06	0.09	0.11	—	—
$\text{Lu}_2\text{O}_3$	—	—	0.10	0.12	0.20
$\text{Sc}_2\text{O}_3$	—	0.09	0.16	0.23	—

NOTES: 1. Time at temperature approximately 350 hours.  
2. Specimens of each composition oxidized at 900°C for 41 hours and at 1000°C for 192 hours did not exhibit any significant weight change. (Weighing balance sensitivity was  $\pm 0.1$  mg.)

20. CHEONG, D-S., and SANDERS, W. A. *High Temperature Deformation and Microstructural Analysis for  $\text{Si}_3\text{N}_4$ - $\text{Sc}_2\text{O}_3$* . NASA Tech. Mem. 103239, NASA Lewis Research Center, Cleveland, OH, August 1990.

## SUMMARY AND CONCLUSIONS

$\text{Si}_3\text{N}_4$  can be fully densified with additions of  $\text{Lu}_2\text{O}_3$ ,  $\text{Er}_2\text{O}_3$ ,  $\text{Yb}_2\text{O}_3$ , or  $\text{Dy}_2\text{O}_3$ . The pyrosilicate phase,  $(\text{RE}_2\text{Si}_2\text{O}_7)$ , was formed with the  $\text{Lu}_2\text{O}_3$ ,  $\text{Er}_2\text{O}_3$ , and  $\text{Yb}_2\text{O}_3$  dopants while a phase which appears to be an N-apatite  $[\text{Dy}_5(\text{SiO}_4)_3\text{N}]$ , crystallized during high temperature testing of the  $\text{Dy}_2\text{O}_3$ -doped specimens. However,  $\text{Dy}_2\text{Si}_2\text{O}_7$  can be formed with appropriate processing conditions.

Hardness and creep resistance of the materials examined generally increased with decreasing ionic radius of the rare earth used for doping, the exception being the  $\text{Yb}_2\text{O}_3$ -doped  $\text{Si}_3\text{N}_4$  which exhibited the lowest hardness and creep resistance of the materials tested in the study. However, another explanation for the levels of hardness and creep resistance observed may involve the solubility of nitrogen in the grain boundary phases and its effect on eutectic temperatures and mechanical properties of phases formed in the  $\text{Si}_3\text{N}_4$ - $\text{RE}_2\text{O}_3$ - $\text{SiO}_2$  systems.

Permanent strain values ( $<1\%$ ) were determined for each  $\text{Si}_3\text{N}_4$ -rare earth composition tested under 300 MPa flexural stress for up to approximately 350 hours at temperatures of  $1200^\circ\text{C}$  to  $1400^\circ\text{C}$ . The  $\text{Lu}_2\text{O}_3$ -doped  $\text{Si}_3\text{N}_4$  exhibited the most resistance to high temperature creep up to the highest test temperature,  $1400^\circ\text{C}$ . Similarities in the slopes of semilogarithmic plots of permanent strain ( $\epsilon$ ) versus  $T$ , for each composition, suggest that creep was controlled by a common mechanism.

## ACKNOWLEDGMENT

The author thanks G. Gilde for assisting with the hardness/indentation toughness measurements, R. Hinxman for XRD data, A. Zani for polished specimen preparation, P. Wong for SEM microscopy, and L. Tardiff for ultrasonic modulus measurements.

# DISTRIBUTION LIST

No. of Copies	To
1	Office of the Under Secretary of Defense for Research and Engineering, The Pentagon, Washington, DC 20301
	Commander, U.S. Army Laboratory Command, 2800 Powder Mill Road, Adelphi, MD 20783-1145
1	ATTN: AMSLC-IM-TL
1	AMSLC-CT
	Commander, Defense Technical Information Center, Cameron Station, Building 5, 5010 Duke Street, Alexandria, VA 22304-6145
2	ATTN: DTIC-FDAC
1	MIAC/CINDAS, Purdue University, 2595 Yeager Road, West Lafayette, IN 47905
	Commander, Army Research Office, P.O. Box 12211, Research Triangle Park, NC 27709-2211
1	ATTN: Information Processing Office
	Commander, U.S. Army Materiel Command, 5001 Eisenhower Avenue, Alexandria, VA 22333
1	ATTN: AMCSCI
	Commander, U.S. Army Materiel Systems Analysis Activity, Aberdeen Proving Ground, MD 21005
1	ATTN: AMXSY-MP, H. Cohen
	Commander, U.S. Army Missile Command, Redstone Scientific Information Center, Redstone Arsenal, AL 35898-5241
1	ATTN: AMSMI-RD-CS-R/Doc
1	AMSMI-RLM
	Commander, U.S. Army Armament, Munitions and Chemical Command, Dover, NJ 07801
1	ATTN: Technical Library
	Commander, U.S. Army Natick Research, Development and Engineering Center, Natick, MA 01760-5010
1	ATTN: Technical Library
	Commander, U.S. Army Satellite Communications Agency, Fort Monmouth, NJ 07703
1	ATTN: Technical Document Center
	Commander, U.S. Army Tank-Automotive Command, Warren, MI 48397-5000
1	ATTN: AMSTA-ZSK
1	AMSTA-TSL, Technical Library
	Commander, White Sands Missile Range, NM 88002
1	ATTN: STEWS-WS-VT
	President, Airborne, Electronics and Special Warfare Board, Fort Bragg, NC 28307
1	ATTN: Library
	Director, U.S. Army Ballistic Research Laboratory, Aberdeen Proving Ground, MD 21005
1	ATTN: GLCBR-TSB-S (STINFO)
	Commander, Dugway Proving Ground, Dugway, UT 84022
1	ATTN: Technical Library, Technical Information Division
	Commander, Harry Diamond Laboratories, 2800 Powder Mill Road, Adelphi, MD 20783
1	ATTN: Technical Information Office
	Director, Benet Weapons Laboratory, LCWSL, USA AMCCOM, Watervliet, NY 12189
1	ATTN: AMSMC-LCB-TL
1	AMSMC-LCB-R
1	AMSMC-LCB-RM
1	AMSMC-LCB-RP
	Commander, U.S. Army Foreign Science and Technology Center, 220 7th Street, N.E., Charlottesville, VA 22901-5396
3	ATTN: AIFRTC, Applied Technologies Branch, Gerald Schlessinger

No. of Copies	To
1	Plastics Technical Evaluation Center, (PLASTEC), ARDEC, Bldg. 355N, Picatinny Arsenal, NJ 07806-5000
	Commander, U.S. Army Aeromedical Research Unit, P.O. Box 577, Fort Rucker, AL 36360
1	ATTN: Technical Library
	Commander, U.S. Army Aviation Systems Command, Aviation Research and Technology Activity, Aviation Applied Technology Directorate, Fort Eustis, VA 23604-5577
1	ATTN: SAVDL-E-MOS
	U.S. Army Aviation Training Library, Fort Rucker, AL 36360
1	ATTN: Building 5906-5907
	Commander, U.S. Army Agency for Aviation Safety, Fort Rucker, AL 36362
1	ATTN: Technical Library
	Commander, USACDC Air Defense Agency, Fort Bliss, TX 79916
1	ATTN: Technical Library
1	Clarke Engineer School Library, 3202 Nebraska Ave. North, Ft. Lebnard Wood, MO 65473-5000
	Commander, U.S. Army Engineer Waterways Experiment Station, P. O. Box 631, Vicksburg, MS 39180
1	ATTN: Research Center Library
	Commandant, U.S. Army Quartermaster School, Fort Lee, VA 23801
1	ATTN: Quartermaster School Library
	Naval Research Laboratory, Washington, DC 20375
1	ATTN: Code 5830
1	Dr. G. R. Yoder - Code 6384
	Chief of Naval Research, Arlington, VA 22217
1	ATTN: Code 471
1	Edward J. Morrissey, WRDC/MLTE, Wright-Patterson Air Force, Base, OH 45433-6523
	Commander, U.S. Air Force Wright Research & Development Center, Wright-Patterson Air Force Base, OH 45433-5523
1	ATTN: WRDC/MLLP, M. Forney, Jr.
1	WRDC/MLBC, Mr. Stanley Schulman
	NASA - Marshall Space Flight Center, MSFC, AL 35817
1	ATTN: Mr. Paul Schuerer/EH01
	U.S. Department of Commerce, National Institute of Standards and Technology, Gaithersburg, MD 20899
1	ATTN: Stephen M. Hsu, Chief, Ceramics Division, Institute for Materials Science and Engineering
1	Committee on Marine Structures, Marine Board, National Research Council, 2101 Constitution Ave., S.W., Washington, DC 20413
1	Librarian, Materials Sciences Corporation, 930 Harvest Drive, Suite 300, Blue Bell, PA 19422
1	The Charles Stark Draper Laboratory, 60 Albany Street, Cambridge, MA 02139
	Wyman-Gordon Company, Worcester, MA 01601
1	ATTN: Technical Library
	General Dynamics, Convair Aerospace Division, P.O. Box 748, Fort Worth, TX 75101
1	ATTN: Mfg. Engineering Technical Library
1	Department of the Army, Aerostructures Directorate, MS-266, U.S. Army Aviation R&T Activity - AVSCOM, Langley Research Center, Hampton, VA 23665-5225
1	NASA - Langley Research Center, Hampton, VA 23665-5225
1	U.S. Army Propulsion Directorate, NASA Lewis Research Center, 2100 Brookpark Road, Cleveland, OH 44135-3191
1	NASA - Lewis Research Center, 2100 Brookpark Road, Cleveland, OH 44135-3191
	Director, U.S. Army Materials Technology Laboratory, Watertown, MA 02172-0001
2	ATTN: SIGHT-TML
1	Author

U.S. Army Materials Technology Laboratory,  
Watertown, Massachusetts 02172-0001  
EXAMINING  $\text{Si}_3\text{N}_4$  BASE MATERIALS WITH  
VARIOUS RARE EARTH ADDITIONS -  
George E. Gazza

Technical Report MTL TR 91-45, December 1991, 19 pp -  
illus-tables, D/A Project IL162105AH84

AD  
UNCLASSIFIED  
UNLIMITED DISTRIBUTION  
Key Words

Silicon nitride  
Hot pressing  
Rare earths

Silicon nitride base compositions were prepared by using various rare earth oxide additives and hot pressing the powders to full density. Compositions were primarily explored in  $\text{Si}_3\text{N}_4$ - $\text{SiO}_2$ - $\text{RE}_2\text{Si}_2\text{O}_7$  compatibility regions although other  $\text{Si}_3\text{N}_4$ - $\text{RE}_2\text{O}_3$  reactions were also investigated. Hot pressing densification data and high temperature behavior of the various silicon nitride-rare earth compositional systems are examined.

U.S. Army Materials Technology Laboratory,  
Watertown, Massachusetts 02172-0001  
EXAMINING  $\text{Si}_3\text{N}_4$  BASE MATERIALS WITH  
VARIOUS RARE EARTH ADDITIONS -  
George E. Gazza

Technical Report MTL TR 91-45, December 1991, 19 pp -  
illus-tables, D/A Project IL162105AH84

AD  
UNCLASSIFIED  
UNLIMITED DISTRIBUTION  
Key Words

Silicon nitride  
Hot pressing  
Rare earths

Silicon nitride base compositions were prepared by using various rare earth oxide additives and hot pressing the powders to full density. Compositions were primarily explored in  $\text{Si}_3\text{N}_4$ - $\text{SiO}_2$ - $\text{RE}_2\text{Si}_2\text{O}_7$  compatibility regions although other  $\text{Si}_3\text{N}_4$ - $\text{RE}_2\text{O}_3$  reactions were also investigated. Hot pressing densification data and high temperature behavior of the various silicon nitride-rare earth compositional systems are examined.

U.S. Army Materials Technology Laboratory,  
Watertown, Massachusetts 02172-0001  
EXAMINING  $\text{Si}_3\text{N}_4$  BASE MATERIALS WITH  
VARIOUS RARE EARTH ADDITIONS -  
George E. Gazza

Technical Report MTL TR 91-45, December 1991, 19 pp -  
illus-tables, D/A Project IL162105AH84

AD  
UNCLASSIFIED  
UNLIMITED DISTRIBUTION  
Key Words

Silicon nitride  
Hot pressing  
Rare earths

Silicon nitride base compositions were prepared by using various rare earth oxide additives and hot pressing the powders to full density. Compositions were primarily explored in  $\text{Si}_3\text{N}_4$ - $\text{SiO}_2$ - $\text{RE}_2\text{Si}_2\text{O}_7$  compatibility regions although other  $\text{Si}_3\text{N}_4$ - $\text{RE}_2\text{O}_3$  reactions were also investigated. Hot pressing densification data and high temperature behavior of the various silicon nitride-rare earth compositional systems are examined.

U.S. Army Materials Technology Laboratory,  
Watertown, Massachusetts 02172-0001  
EXAMINING  $\text{Si}_3\text{N}_4$  BASE MATERIALS WITH  
VARIOUS RARE EARTH ADDITIONS -  
George E. Gazza

Technical Report MTL TR 91-45, December 1991, 19 pp -  
illus-tables, D/A Project IL162105AH84

AD  
UNCLASSIFIED  
UNLIMITED DISTRIBUTION  
Key Words

Silicon nitride  
Hot pressing  
Rare earths

Silicon nitride base compositions were prepared by using various rare earth oxide additives and hot pressing the powders to full density. Compositions were primarily explored in  $\text{Si}_3\text{N}_4$ - $\text{SiO}_2$ - $\text{RE}_2\text{Si}_2\text{O}_7$  compatibility regions although other  $\text{Si}_3\text{N}_4$ - $\text{RE}_2\text{O}_3$  reactions were also investigated. Hot pressing densification data and high temperature behavior of the various silicon nitride-rare earth compositional systems are examined.



**END  
FILMED**

**DATE:**

*1-92*

**DTIC**